The Ewing's sarcoma oncoprotein EWS/FLI induces a p53-dependent growth arrest in primary human fibroblasts

Stephen L. Lessnick,[1,2] Caroline S. Dacwag,[1] and Todd R. Golub[1,2,3,4]

[1]Department of Pediatric Oncology, Dana-Farber Cancer Institute, Boston, Massachusetts 02115
[2]Division of Hematology/Oncology, Children's Hospital, Boston, Massachusetts 02115
[3]Whitehead/MIT Center for Genome Research, Cambridge, Massachusetts 02142
[4]Correspondence: golub@genome.wi.mit.edu

Summary

Ewing's sarcoma is associated with a fusion between the *EWS* and *FLI1* genes, forming an EWS/FLI fusion protein. We developed a system for the identification of cooperative mutations in this tumor through expression of EWS/FLI in primary human fibroblasts. Gene expression profiling demonstrated that this system recapitulates many features of Ewing's sarcoma. EWS/FLI-expressing cells underwent growth arrest, suggesting that growth arrest-abrogating collaborative mutations may be required for tumorigenesis. Expression profiling identified transcriptional upregulation of p53, and the growth arrest was rescued by inhibition of p53. These data support a role for p53 as a tumor suppressor in Ewing's sarcoma and demonstrate the use of transcriptional profiling of model systems in the identification of cooperating mutations in human cancer.

Introduction

The study of solid tumor formation in pediatrics has made great strides in recent years by the identification of recurrent chromosomal alterations involved in these tumors (reviewed in Sorensen and Triche, 1996). Ewing's sarcoma serves as a paradigm for this tumor class, since virtually all Ewing's sarcomas contain one of a small group of chromosomal translocations (reviewed in Kim and Pelletier, 1999; Kovar, 1998). The most common translocation is the t(11;22)(q24;q12), which results in a fusion protein containing the amino terminus of the EWS protein joined to the carboxyl terminus of the FLI1 protein, an ETS transcription factor (Dellatre et al., 1992). It is believed that the consequence of this fusion is to replace the weak transcriptional activation domain of FLI1 with a strong transcriptional activation domain from EWS (Lessnick et al., 1995; May et al., 1993b). The other Ewing's sarcoma-associated translocations fuse the amino terminus of EWS to the DNA binding domain of other ETS family transcription factors.

Although the cell of origin of Ewing's sarcoma is not known, the transforming potential of EWS/FLI has been demonstrated in NIH 3T3 fibroblasts, where it induces colony formation in soft agar and forms tumors when injected in immunodeficient mice (May et al., 1993a; Teitell et al., 1999). These tumors share the "small round blue cell" and neural differentiation properties of human Ewing's sarcomas, suggesting that the morphology of the tumor may be governed by the EWS/FLI oncogene itself, rather than by the tumor's cell of origin (Teitell et al., 1999). Importantly, other cell types (e.g., Rat-1 fibroblasts, Ncm1, CTR, and the NIH 3T3-derived line YAL-7) are not transformable by EWS/FLI, suggesting that the fusion protein may not be sufficient for transformation (Arvand et al., 1998, and references therein). The full spectrum of EWS/FLI-collaborating mutations, however, is not known, and the requirements for transformation by EWS/FLI in primary cells is poorly understood.

To address the functional consequences of EWS/FLI in primary cells, we report here the establishment of telomerase-immortalized human primary fibroblasts conditionally expressing the fusion protein. These cells underwent EWS/FLI-induced growth arrest, consistent with the notion that tumorigenesis requires the acquisition of additional mutations that abrogate this growth arrest response. To work toward the elucidation of this multistep oncogenic process, transcriptional profiling coupled with functional validation studies were performed. These experiments indicated that this growth arrest is p53 dependent, supporting the importance of p53 loss of function in the pathogenesis of Ewing's sarcoma and demonstrating the feasibility of this experimental approach to finding cooperative mutations in cancer.

SIGNIFICANCE

Cancer arises as a consequence of multiple cooperating genetic events. The unique character and early age of onset of pediatric tumors suggests that there may be qualitative and/or quantitative differences in the alterations required as compared to adult tumors, but this has not been systematically evaluated. Such an evaluation has been hampered by the difficulty in identification of cooperative mutations involved in these tumors. We developed a system to identify cooperative mutations in the pediatric tumor Ewing's sarcoma. We describe a generalizable approach to the validation of this experimental system using microarray-based transcriptional profiling of primary patient samples. The utility of this approach is demonstrated by the identification and functional validation of p53 as a tumor suppressor in Ewing's sarcoma.

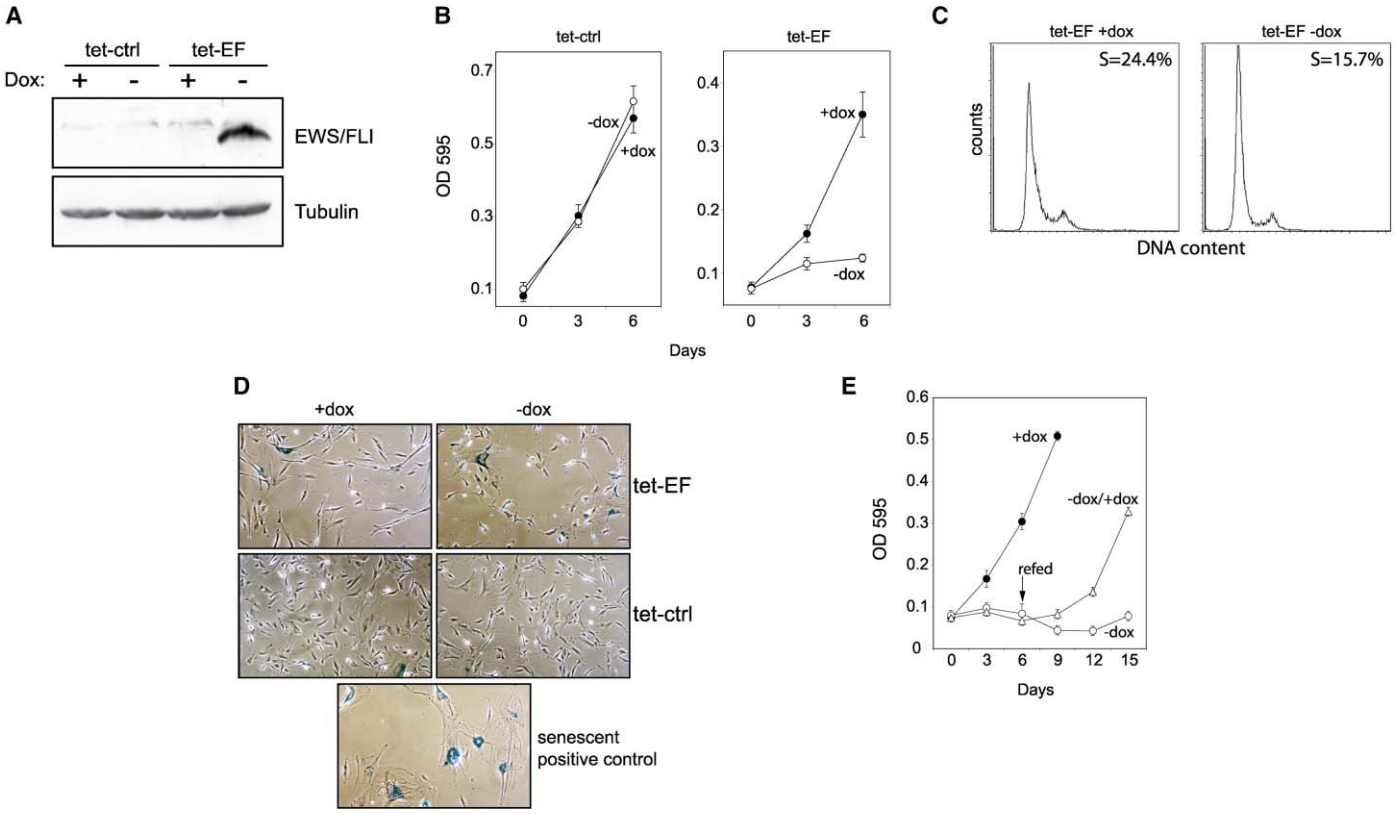

Figure 1. Growth phenotype of tet-EF cells

A: Tet-EF cells expressed EWS/FLI (as detected by Western blot with anti-FLAG antibody) following removal of doxycycline from the culture media. Tet-ctrl cells do not contain an inducible cDNA. Tubulin staining demonstrates equal loading of samples. **B:** The growth of tet-EF cells was significantly repressed by the presence of EWS/FLI expression (i.e., without doxycycline; open circles) as compared to the absence of EWS/FLI expression (i.e., with doxycycline; closed circles). The optical density at 595 nm (OD 595) is proportional to the cell number at each time point. Error bars indicate the standard deviations of triplicate samples. **C:** Cell cycle analysis of tet-EF cells reveals a decrease in the S phase percentage from 24.4% to 15.7% when EWS/FLI is expressed (i.e., without doxycycline). **D:** SA-β-gal staining of tet-EF cells does not demonstrate significant differences in the presence or absence of doxycycline. Although the total number of cells is decreased in the induced tet-EF sample (−dox) as compared to the uninduced tet-EF cell sample (+dox), the absolute number of cells staining positively for SA-β-gal is identical between the two. A senescent positive control (tet-ctrl cells expressing SV40 small T antigen) is shown for comparison. **E:** The growth arrest of tet-EF cells is reversible, as demonstrated by resumption of growth when EWS/FLI expression was inhibited by the readdition of doxycycline to the growth media. The standard deviations from triplicate samples are represented by error bars.

Results

Growth phenotype of inducible EWS/FLI

To study the biological effects of EWS/FLI in primary human cells, human neonatal foreskin fibroblasts were infected with a retrovirus harboring the human telomerase (hTERT) cDNA to provide for an extended life span without karyotypic abnormalities. These cells were then engineered to express EWS/FLI under the control of a tetracycline-repressible element and were designated tet-EF cells (Figure 1A). A control cell line (tet-ctrl cells) lacking the EWS/FLI cDNA was similarly generated.

Growth curves were generated using tet-EF and tet-ctrl cells following the withdrawal of doxycycline (Figure 1B). Control cells grew similarly in the presence or absence of doxycycline. In contrast, tet-EF cells exhibited a dramatic inhibition of population growth when induced to express EWS/FLI. An independent EWS/FLI-inducible clone demonstrated an identical growth-suppressive response to EWS/FLI (data not shown).

Cell cycle analysis of tet-EF cells demonstrated a decrease in S phase following induction of EWS/FLI (Figure 1C). There was no evidence of a sub-G_0 population to suggest an apoptotic response, such as that seen with c-*myc* expression in nontransformed fibroblasts (reviewed in Prendergast, 1999). In situ staining with FITC-VAD-fmk, gel electrophoresis to detect genomic DNA laddering, DAPI staining of nuclei to detect characteristic nuclear condensation, and annexin V staining, a hallmark of apoptosis, similarly failed to demonstrate an apoptotic response to EWS/FLI expression (data not shown). Additionally, in contrast to the effects of RAS expression in primary cells (Serrano et al., 1997), EWS/FLI did not induce a senescent phenotype, as demonstrated by the absence of the typical morphologic changes of cellular senescence and the absence of senescence-associated β-galactosidase activity (Figure 1D). Furthermore, the EWS/FLI-induced growth arrest was completely reversed by the readdition of doxycycline, thereby repressing EWS/FLI expression (Figure 1E). Taken together, these results indicate that EWS/FLI induces a reversible, nonsenescent, nonapoptotic growth arrest in primary cells.

Validation of tet-EF model

The growth arrest induced by EWS/FLI is consistent with the hypothesis that additional mutations are required to abrogate

this default growth arrest pathway before Ewing's tumors could form. One potential concern, however, is that the tet-EF fibroblast system might not reflect the biology of naturally occurring Ewing's sarcoma. To address this, we compared tet-EF cells to Ewing's sarcoma cell lines and tumor samples.

Western blot analysis showed that the expression of EWS/FLI protein is similar in tet-EF cells as compared to cell lines derived from Ewing's sarcoma patient samples (Figure 2A). Given this comparable level of expression, it is unlikely that the growth arrest observed in EWS/FLI-expressing tet-EF cells is simply a result of overexpression of the fusion protein.

Tet-EF cells induced to express EWS/FLI were next analyzed on DNA microarrays containing probes for approximately 12,600 named genes and expressed-sequence tags (see Supplementary Information at http://www.genome.wi.mit.edu/cancer/Ewings). Among the genes induced by EWS/FLI in these experiments was *MIC2*, a marker of Ewing's sarcoma used in routine clinical practice (Figure 2B; Ambros et al., 1991; Fellinger et al., 1991). This result supports the validity of the cell culture system for the study of EWS/FLI.

To further explore the validity of this model system, we compared the list of EWS/FLI-induced genes to the gene expression profiles of Ewing's sarcoma patient samples. The 12,600 gene oligonucleotide microarray data generated herein were compared to the 2308 gene cDNA microarray data of Khan et al., which represent 63 small round blue cell tumors and cell lines, including 23 Ewing's sarcomas, 8 Burkitt's lymphomas, 12 neuroblastomas, and 20 rhabdomyosarcomas (Khan et al., 2001). Permutation testing of the oligonucleotide array data revealed that 117 probes were reproducibly induced by EWS/FLI in tet-EF cells ($p < 0.01$; Figure 2C). Analysis of the patient samples identified 686 probes that were statistically significant markers of Ewing's sarcoma ($p < 0.01$; Figure 2C). Strikingly, 54 (46.2%) of the 117 genes that were induced by the EWS/FLI fusion in tet-EF cells were also Ewing's-specific markers, far beyond what would have been expected by chance alone ($p < 0.0001$; Figure 2D). We similarly identified genes that were specific to Burkitt's lymphoma, neuroblastoma, and rhabdomyosarcoma, and compared these to the EWS/FLI-induced genes in tet-EF cells (Figures 2C and 2D). No significant molecular similarity between the tet-EF cells and these other tumor types was observed (Figure 2D). These results demonstrate that tet-EF cells have molecular features that are similar to Ewing's sarcoma, and thus they confirm the suitability of tet-EF cells as a model of Ewing's sarcoma.

Molecular consequence of EWS/FLI expression

We next explored the mechanism by which EWS/FLI induces growth arrest, reasoning that genes involved in that process would be candidates for collaborating mutations in Ewing's tumorigenesis. For this purpose, we turned again to the gene expression consequences of EWS/FLI induction in tet-EF cells. EWS/FLI-regulated genes were clustered using self-organizing maps (SOM) in order to capture the predominant patterns of gene expression (Figure 3A; Tamayo et al., 1999). The data could be divided into three major groups: those that were downregulated in response to EWS/FLI (cluster 0; 347 genes), those that were upregulated (cluster 2; 214 genes), and those that had more variable expression patterns (cluster 1; 134 genes). A complete list of these genes can be found in Supplemental Information at http://www.genome.wi.mit.edu/cancer/Ewings.

Many of the genes downregulated by EWS/FLI are involved in cell cycle progression and DNA replication, including multiple cyclins (*CCNA2, CCNB1, CCNE1,* and *CCNE2*), a cyclin-dependent kinase (*CDC2*), DNA polymerase subunits (*POLA*, *POL2A*, *POLE2,* and *PCNA*), replication factor subunits (*RFC2, RFC3, RFC4,* and *RFC5*), DNA primase subunits (*PRIM1* and *PRIM2A*), and the Ki-67 antigen (*MKI67*). This transcriptional readout is consistent with the cell cycle arrest that ensues following EWS/FLI expression.

Among EWS/FLI upregulated genes were frizzled-1 (*FZD1*), *FRAT2* (a GSK binding protein), and *MYC*, suggesting that modulation of the WNT signaling pathway may be occurring in these cells, and consistent with the observation of elevated levels of c-MYC in Ewing's sarcoma (McKeon et al., 1988). Upregulation of the PDGF-receptor-β (*PDGFRB*), the PI-3-kinase p85 subunit (*PIK3R1*), and multiple MAP-kinase pathway genes (such as *MAPK10*, *MAP2K5*, and *MAPKAPK2*) suggests that EWS/FLI may modulate multiple points in receptor tyrosine-kinase pathways. Interestingly, induction of *VEGF* expression by EWS/FLI suggests a possible mechanism for the extensive tumor angiogenesis observed in Ewing's sarcoma. An additional group of EWS/FLI-induced genes include *p53* (*TP53*), *FAS*/*APO* (*TNFRSF6*), *CDKN1C*, *TGFB1*, and *TIMP3*—all of which are associated with tumor growth inhibition. We hypothesized that these genes represent cell-autonomous tumor-suppressive responses to oncogenic stress. One implication of this hypothesis is that Ewing's sarcoma tumor cells have bypassed these cellular responses to allow for unrestricted cell growth. As described below, the plausibility of this hypothesis was functionally validated for one of these genes—*p53*.

EWS/FLI induction of p53

p53 represents an attractive candidate to explain EWS/FLI-mediated growth arrest, since p53 transcript levels were more highly correlated with EWS/FLI expression than any of the other 12,600 genes on the array, and increases in p53 function are thought to be central to the growth arrest and increased cell death observed in primary cells expressing oncogenes (Serrano et al., 1997; Zindy et al., 1998). Quantitative, real-time PCR experiments showed induction of p53 mRNA levels that were consistent with the microarray findings (Figure 3B). Western blot analysis further demonstrated significant increases in p53 levels following EWS/FLI induction (Figure 4A). Similar increases in the p53 target p21 support the notion that the increase in p53 levels was functionally significant (see Figure 4C).

Oncogene expression in primary murine fibroblasts often activate the p53 tumor suppressor via increases in the p19ARF protein (p14ARF in human cells), which results in increased stability of p53 and accumulation of active protein (Bates et al., 1998; Damalas et al., 2001; de Stanchina et al., 1998; Palmero et al., 1998; Pomerantz et al., 1998; Zhang et al., 1998; Zindy et al., 1998). Posttranslational regulation of p53 levels are similarly observed in MDM2-overexpressing cells (Haupt et al., 1997; Kubbutat et al., 1997). The observed increases in p53 mRNA levels in tet-EF cells, however, raised the possibility that the regulation of p53 in this system may occur transcriptionally. In support of this, we observed no increase in p14ARF protein levels in response to EWS/FLI expression and minimal change in MDM2 protein levels (Figure 4A). Quantitative, real-time PCR experiments demonstrated no increase in p14ARF mRNA levels and, in fact, demonstrated 3-fold decrease in mRNA levels, in good agreement with the Western blot data (data not shown).

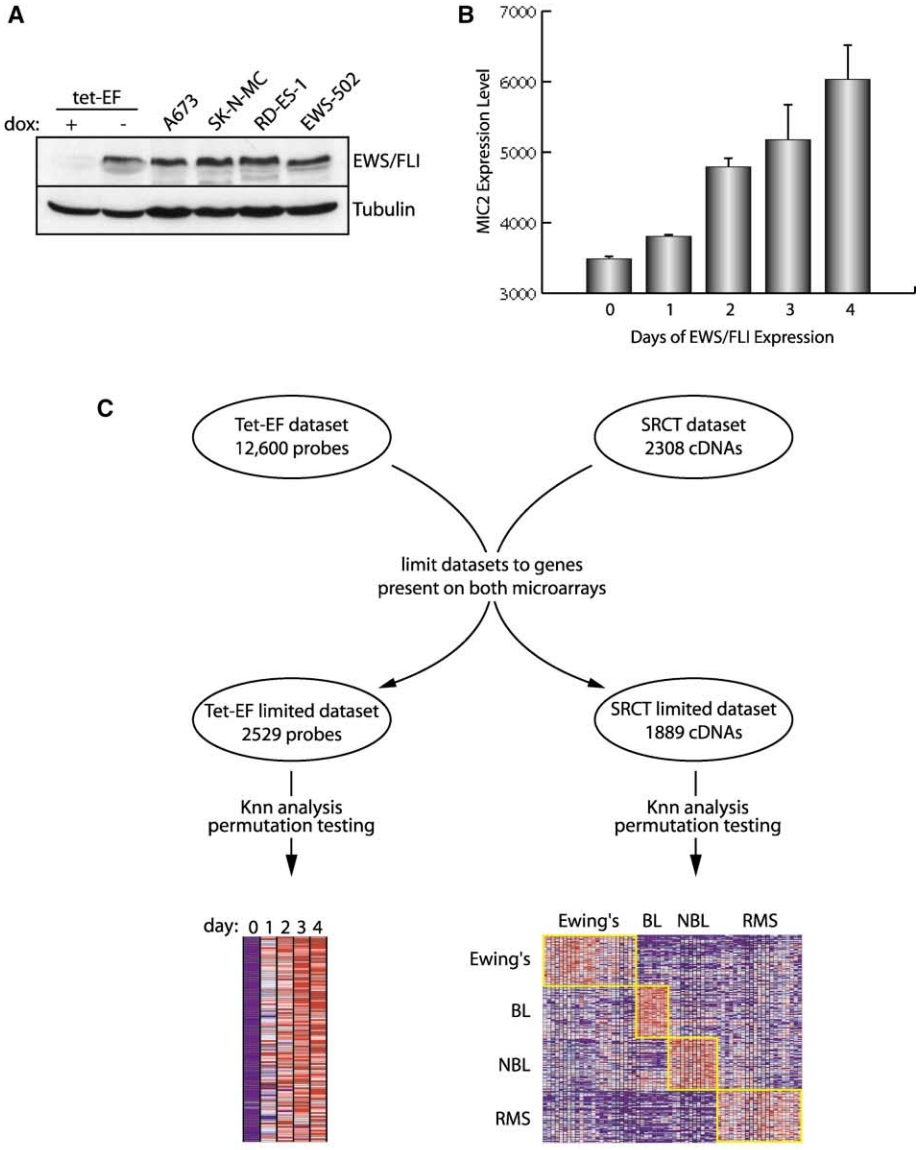

Figure 2. Tet-EF cells have molecular features that are similar to Ewing's sarcoma

A: Western blot analysis using an anti-FLI-1 antibody demonstrates that the level of EWS/FLI expressed in the absence of doxycycline is similar to the levels of EWS/FLI protein expressed by the Ewing's sarcoma cell lines A673, SK-N-MC, RD-ES-1, and EWS-502. Tubulin is shown as a loading control. **B:** Microarray-detected *MIC2* mRNA expression levels increase following EWS/FLI expression. **C:** The oligonucleotide microarray data for tet-EF cells expressing EWS/FLI were compared to the publicly-available cDNA microarray expression data for pediatric small round cell tumors (SRCT) (Khan et al., 2001), including Ewing's sarcoma, Burkitt's lymphoma (BL), neuroblastoma (NBL), and rhabdomyosarcoma (RMS). Oligonucleotide probes and cDNAs were first mapped to their Unigene clusters, and clusters that were present on both microarray platforms were identified. Data from the common clusters were used for the subsequent analysis. The different numbers of probes/cDNAs obtained for each data set is a result of different amounts of redundancy present on each platform. K-nearest neighbor (Knn) analysis and permutation testing was used to identify those genes that increase following EWS/FLI expression in tet-EF cells (left; n = 117 at 99% significance level). A representative experiment is shown. Each column represents the day following induction of EWS/FLI. Each row represents a different gene. The same method was used to identify marker genes that are more highly expressed in each SRCT type than expected by chance alone (right; the top 50 genes are shown for each tumor type). For both panels, expression levels are normalized such that the mean is 0 and the standard deviation is 1. Expression levels above the mean are red, and those below the mean are blue. **D:** EWS/FLI-regulated genes are more overlapping with Ewing's sarcoma markers than would be expected by chance alone ($p < 0.0001$). For each tumor type shown, the number of probes that pass permutation testing at the 99% significance level is shown. Chi-square analysis was used to generate the p values.

D

tumor type	# significant probes	expected overlap	observed overlap	p value
Ewing's sarcoma	686	32	54	<0.0001
Burkitt's lymphoma	744	34	27	0.23
Neuroblastoma	772	36	26	0.12
Rhabdomyosarcoma	931	43	42	0.92

Finally, pulse-chase experiments demonstrated that p53 half-life was not prolonged following EWS/FLI induction (Figure 4B). Importantly, introduction of p14ARF or p53 expression by retroviral transduction led to the anticipated increases in both MDM2 and p53 levels (Figure 4A; Stott et al., 1998). Taken together, these results demonstrate that tet-EF cells carry a functional ARF-MDM2-p53 axis, but this pathway is not activated in response to EWS/FLI expression. Thus, EWS/FLI expression results in increased p53 levels because of transcriptional upregulation, rather than posttranslational mechanisms.

Growth arrest is p53 dependent

We next determined whether p53 induction was critical for the observed growth arrest phenotype following EWS/FLI induction.

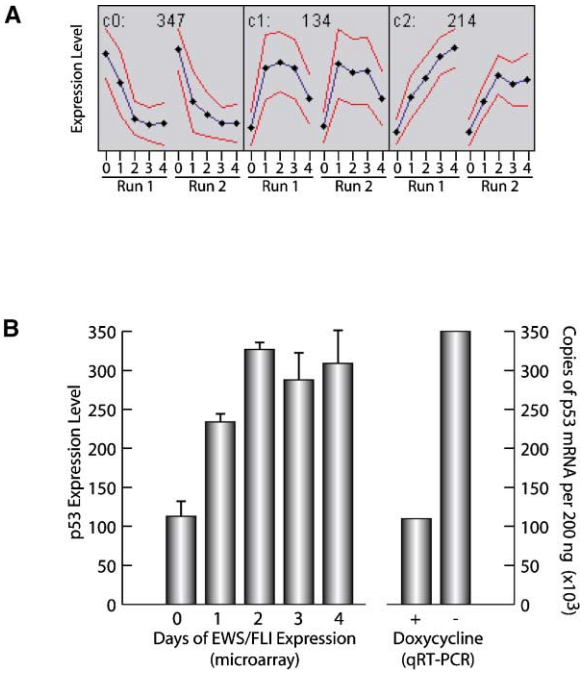

Figure 3. EWS/FLI upregulates p53 transcription

A: Self-organized map analysis of tet-EF cells expressing EWS/FLI. The tet-EF cell microarray data was initially filtered to limit the data set to those genes that demonstrated at least 2.5-fold changes in two or more time points as compared to day 0. Genes were then grouped into three clusters (a 3 × 1 SOM). The mean expression level of each clustered time point is represented in blue, and the standard deviations are in red. Independent duplicate EWS/FLI inductions in tet-EF cells are represented, and the day of induction of each point is indicated. Cluster 0 (c0) represents downregulated genes, cluster 2 (c2) represents upregulated genes, and cluster 1 (c1) represents genes with intermediate/indeterminate patterns. **B:** Quantitative real-time PCR (qRT-PCR) of an independent sample of tet-EF cells expressing EWS/FLI demonstrates similar increase in p53 mRNA as compared to the microarray analysis. The p53 mRNA expression level from the microarray is plotted on the left, and the levels as determined by qRT-PCR is shown on the right. The microarray data represents the mean of both runs with the standard deviations indicated. The qRT-PCR analysis was performed on a single independent sample pair.

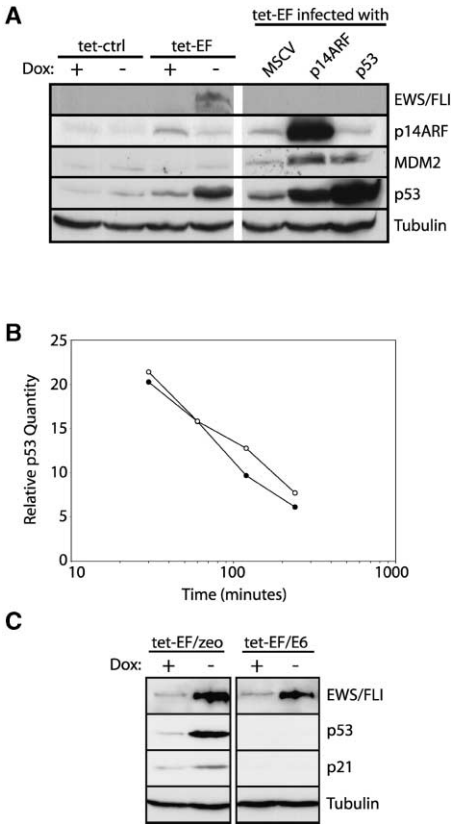

Figure 4. EWS/FLI increases p53 protein levels

A: Western blot analysis of the p53 pathway in tet-EF cells following 3 days of induced EWS/FLI expression. EWS/FLI expression results in increased p53 protein levels without increased p14ARF levels or significant alterations in MDM2 levels. Infection of tet-EF cells with a p14ARF retrovirus demonstrates that p14ARF is able to mediate increased p53 levels. Increased MDM2 levels are observed following infection of either p14ARF or p53 retroviruses, as has been previously reported (Stott et al., 1998, and references therein). Tubulin is shown as a loading control. **B:** Pulse-chase analysis of p53 protein stability in the presence of EWS/FLI expression (open circles, without doxycycline) or in the absence of EWS/FLI expression (closed circles, with doxycycline). Relative p53 quantities (as determined using a phosphor imager) are shown plotted against time (on a logarithmic scale). **C:** Western blot analysis of tet-EF/E6 cells and tet-EF/zeo control cells following 3 days of induced EWS/FLI expression. Increases in p53 and p21 following EWS/FLI expression are abrogated by coexpression of E6 protein. Tubulin is shown as a loading control.

We utilized the E6 protein of human papillomavirus HPV16 as an inhibitor of p53 (Vousden, 1993). Polyclonal populations of tet-EF cells stably expressing E6 (tet-EF/E6 cells) were generated by retroviral gene transfer. Control cells lacking E6 (tet-EF/zeo) were similarly derived.

E6 expression in tet-EF cells led to expected diminution of basal p53 protein levels and was able to completely inhibit increased p53 levels seen with EWS/FLI induction (Figure 4C). Additionally, increases in p21 were also inhibited by the presence of the E6 protein (Figure 4C). Importantly, EWS/FLI expression levels were similar in the two cell types (Figure 4C).

The growth characteristics of tet-EF/E6 cells are shown (Figure 5A). Whereas tet-EF/zeo cells undergo growth arrest in response to EWS/FLI induction, this growth arrest was completely abrogated by E6 expression. A dominant-negative allele of p53 demonstrated a similar bypass in the growth arrest response to EWS/FLI (see below). These experiments indicate that p53 is a critical mediator of EWS/FLI growth arrest.

Multistep process of transformation

We next asked whether inhibition of p53 was sufficient for EWS/FLI-mediated transformation. Tet-EF/E6 cells were plated in soft agar in the presence and absence of doxycycline. No colonies formed when tet-EF/E6 cells were induced to express EWS/FLI protein (Figure 5B). Importantly, these cells do become transformed through coexpression of HPV E6 and E7, SV40 small T antigen, and RAS^{V12} (Figure 5B; Hahn et al., 2002). Interestingly, the colony-forming potential of these cells is inhibited by expression of EWS/FLI, suggesting that additional tumor-suppressive pathways may be operative in these cells. To examine this possibility, 3T5 growth assays were performed with tet-EF/E6 cells. Whereas E6 blocked an early, p53-dependent growth arrest, subsequent p53-independent growth inhibition was then encountered (Figure 5C). A dominant-negative allele of p53,

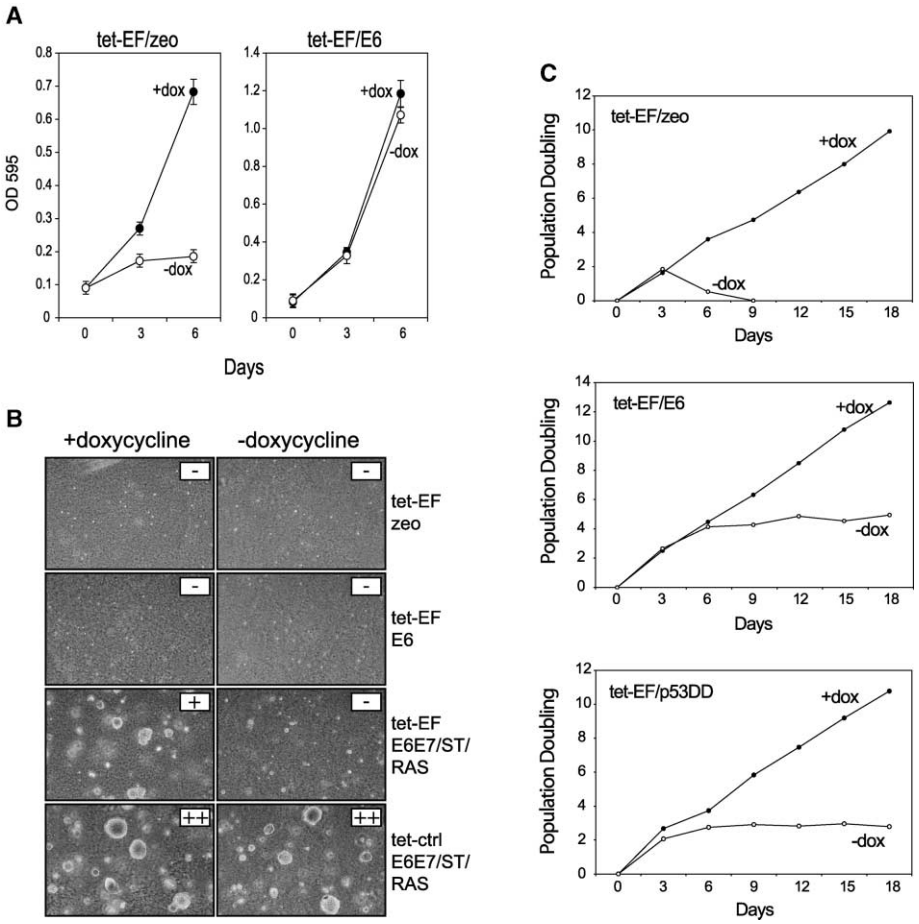

Figure 5. EWS/FLI-mediated growth arrest is p53 dependent

A: Growth curve analysis of tet-EF/E6 cells and tet-EF/zeo cells demonstrates bypass of growth arrest in the presence of E6 protein. The optical density at 595 nm is proportional to the cell number at each time point. Error bars demonstrate the standard deviation of triplicate samples. **B:** Soft agar assays demonstrate that EWS/FLI expression does not result in colony formation in the presence of E6 protein. Tet-EF/E6E7/ST/RAS^{V12} cells utilized as a positive control (in the presence of doxycycline) demonstrate that colony formation is suppressed by EWS/FLI expression (in the absence of doxycycline). Tet-ctrl/E6E7/ST/RAS^{V12} cells form colonies in the presence and absence of doxycycline. Photomicrographs were taken 3 weeks following plating. The plus and minus signs indicate the qualitative level of transformation. **C:** Passage on a 3T5 schedule reveals that while tet-EF/E6 cells bypass an early growth arrest, they undergo a secondary arrest after two passages. Tet-EF/zeo cells are shown for comparison. Tet-EF/p53DD cells demonstrate a similar pattern of delayed growth arrest to the tet-EF/E6 cells, thus proving that the effects of E6 are mediated by p53 inhibition, rather than a non-p53-mediated function of E6.

p53DD (Shaulian et al., 1992), similarly abrogated the growth arrest phenotype, suggesting that the effects observed with HPV E6 are a result of its p53-inhibitory functions, rather than its p53-independent activities. Taken together, these data suggest that the pathogenesis of Ewing's sarcoma requires not only abrogation of the p53 pathway, but also requires mutations in genes leading to the abrogation of an additional, as yet uncharacterized growth-suppressive pathway.

Discussion

We have demonstrated the potential for deciphering the multistep pathogenesis of Ewing's sarcoma by integrating transcriptional profiling data from model systems and patient tumor samples with functional assays in model systems. We identified p53 as a potential tumor suppressor in Ewing's sarcoma through this method. A role for p53 alterations in Ewing's sarcoma is supported by the clinical literature, and thus lends validity to this approach. Mutations in *p53* have been detected in 5%–20% of Ewing's sarcoma tumor samples (Kovar et al., 1993; Patino-Garcia and Sierrasesumaga, 1997). Amplification of *MDM2* and deletions of the *CDKN2A* locus (encoding overlapping *INK4A* and *ARF* transcripts) have also been described in Ewing's sarcoma (e.g., Kovar et al., 1997; Ladanyi et al., 1995). Thus, alterations in the p53 *pathway* may be relatively frequent in this tumor.

Activation of tumor suppressor pathways by oncogenic stress is an emerging theme. *RAS, MYC, E1A, E2F1*, and β-catenin (*CTNNB1*) all induce p53-dependent growth-inhibitory responses when expressed in primary murine cells (Bates et al., 1998; Damalas et al., 2001; de Stanchina et al., 1998; Palmero et al., 1998; Zindy et al., 1998). In each of these instances, upregulation of p53 protein levels is thought to be mediated by the ARF-MDM2-p53 axis. Indeed, expression of EWS/FLI in primary *murine* fibroblasts results in a growth arrest with apoptosis that can be circumvented by loss of either p19ARF or p53 (Deneen and Denny, 2001). Importantly, we did not observe activation of the ARF-MDM2 pathway in primary *human* fibroblasts, suggesting that regulation of the p53 tumor suppressor may be different in different organisms. Consistent with this notion, recent work from Sedivy and coworkers has demonstrated that p53 induction by RAS in primary human fibroblasts also occurs in an ARF-independent fashion (Wei et al., 2001). Thus, it would appear that regulation of p53 levels by oncogenic stress in primary human cells utilizes different upstream components than those used in murine cells. In the case of EWS/FLI, transcriptional upregulation of p53 seems to be the predominant mode of regulation. Additional work will be required to determine whether this finding is specific for EWS/FLI, or whether it is a more generalized phenomenon. As many cases of Ewing's sarcoma have no evidence of mutation of the p53 pathway, abrogation of the transcriptional induction of p53

by EWS/FLI represents a potential mechanism of escaping p53-mediated growth control.

While HPV16 E6 effectively rescued the early EWS/FLI-induced growth arrest, a subsequent p53-independent growth arrest was encountered, suggesting that still additional mutations must be acquired in the process of Ewing's sarcoma pathogenesis. Of note, the delayed growth-inhibitory response to EWS/FLI was dominant over not only E6, but also the combination of E6E7, ST, and RAS (and therefore, the transformed phenotype). The transcriptional data provided in this study may allow for the identification of additional genetic alterations required for Ewing's sarcoma development. A number of growth-inhibitory genes were upregulated following EWS/FLI induction in tet-EF cells. Further studies, such as those described in this report, may provide evidence for functional roles of these in the growth arrest of tet-EF cells expressing EWS/FLI and, by inference, for the role of these in the development of Ewing's sarcoma.

It has been recently suggested that loss of the p16-RB pathway allows for stable EWS/FLI expression in primary fibroblasts, suggesting that abrogation of the RB pathway may cooperate with EWS/FLI (Deneen and Denny, 2001). In our human model system, however, RB blockade with HPV E7 did not abrogate EWS/FLI-mediated growth arrest, nor were we able to detect upregulation of p16INK4a protein following EWS/FLI expression in our model system (S.L.L. and T.R.G., unpublished observations). Thus, the p16-RB pathway is not a critical mediator of EWS/FLI growth arrest in tet-EF cells. It seems likely that different cellular backgrounds may emphasize different growth-suppressive pathways and may thus be exploited to gain a more complete understanding of Ewing's sarcoma genesis.

Experimental procedures

Constructs and retroviruses

The human telomerase (hTERT) cDNA was cloned into the pWZL-blastϵ vector, which directs blasticidin resistance. HPV16 E6 and E6E7 cDNAs were PCR amplified from an HPV16 genomic plasmid and cloned into pWZL-zeoϵ vector. FLAG-epitope-tagged EWS/FLI was subcloned into the pREV-TRE vector (Clontech). The cDNAs for p14ARF and wild-type p53 were subcloned into the MSCV-puro vector (Clontech) for retroviral production and into the pBluescript II KS+ vector (Stratagene) for in vitro transcription reactions. The cDNA for p53DD was subcloned into the pBabe-puro vector (Morgenstern and Land, 1990).

Vesicular stomatitis virus-G glycoprotein pseudotyped retroviruses were prepared by transient cotransfection of retroviral vectors with packaging plasmids in either 293-EBNA (Invitrogen) or 293T cells. Infection of target cells was carried out in the presence of 8 μg/ml polybrene.

Cell culture

Primary fibroblasts were prepared from discarded neonatal foreskins and were immortalized by infection with hTERT-pWZL-blastϵ retrovirus and selection with blasticidin (Invitrogen) at population doubling 20. Tet-EF cells were generated by retroviral transduction of pREV-TETOFF (Clontech). Following neomycin selection, a portion of the surviving population was infected with FLAG-EWS/FLI-pREV-TRE retrovirus and subjected to hygromycin selection in the presence of tetracycline. Negative control cells were prepared by introducing an empty pREV-TRE retroviral construct instead of the EWS/FLI-containing construct. Cells were maintained in 10%FCS in DMEM supplemented with 1 μg/ml doxycycline or tetracycline, 300 μg/ml G418, and 100 μg/ml hygromycin.

Induction of EWS/FLI was accomplished by plating the cells in media containing 1 μg/ml tetracycline the day before induction, washing the tet-EF cells three times with phosphate-buffered saline (PBS) on the day of induction, and refeeding with tetracycline-free growth media.

Ewing's sarcoma cell lines A673, SK-N-MC, and RD-ES-1 were obtained from American Type Culture Collection (ATCC) and grown according to ATCC recommendations. The Ewing's sarcoma cell line EWS-502 was grown in 15% FCS in RPMI media.

Immunodetection

The following antibodies were used: M2-anti-FLAG (Stratagene or Sigma); anti-FLI-1 (BD PharMingen 554266); anti-p14ARF (Oncogene Research Products NA70); anti-MDM2 (Oncogene Research Products OP46); anti-p53 (DO-1; Santa Cruz sc-126); anti-p21 (Santa Cruz sc-397); and anti-α-tubulin (Santa Cruz sc-5286).

Growth curves

In triplicate, 2×10^4–3×10^4 cells were plated per well of 12-well plates in media containing tetracycline. On day 0, the cells were induced to express EWS/FLI. Uninduced cells were refed with media containing 1 μg/ml of doxycycline. At the indicated times, the cells were washed, fixed, and stained (Serrano et al., 1997).

Cell cycle analysis

Three days after EWS/FLI induction, cells were fixed in 35% ethanol, washed in PBS, and resuspended in PBS containing propidium iodide and RNase A. Cells were subsequently analyzed by flow cytometry.

Microarray analysis

Tet-EF cells were plated at 1×10^6 cells per 15 cm plate, five plates in total, in tetracycline-containing media. On day 0, one plate of cells was collected, pelleted, and stored frozen in Trizol reagent (Life Technologies). The remaining plates were induced to express EWS/FLI as described above, and each day one plate was collected, pelleted, and stored frozen in Trizol. The entire induction experiment was repeated on a subsequent week. Following collection of the final sample, total RNA was isolated, processed, hybridized to Affymetrix U95Av2 microarrays, and scanned. The expression value for each gene was calculated using Affymetrix GeneChip software. Minor differences in microarray intensity were corrected using a linear scaling method as detailed in the supplemental section. K-nearest neighbor (Knn) analysis and SOMs were performed using our GeneCluster software package available at http://www-genome.wi.mit.edu/cancer/software/software (Golub et al., 1999; Tamayo et al., 1999). Complete data sets, in-depth description of the analysis, and supplemental materials are available at http://www.genome.wi.mit.edu/cancer/Ewings.

Real-time quantitative PCR

Three days after EWS/FLI induction in tet-EF cells, total cellular RNA was prepared and was treated with RNase-free DNase I (Promega). Reactions were prepared using TaqMan One-Step RT-PCR reagents from Applied Biosystems. One-step RT-PCR consisted of an initial incubation at 48°C for 30 min, followed by a denaturation step at 95°C for 10 min and amplification for 40 cycles of 15 s at 95°C and 1 min at 60°C. For each case, 200 ng of total RNA was analyzed. Each experiment included three nontemplate controls to detect any template contamination; a control lacking reverse transcriptase was included for each sample to detect any residual genomic DNA. Standard curves were constructed by serial 10-fold dilutions from 10^7 to 10^3 copies of in vitro transcribed RNA of each gene to be quantified. The reproducibility of the quantitative measurements was evaluated by conducting triplicate PCR assessments. Glyceraldehyde-3-phosphate dehydrogenase (GAPDH) mRNA expression was analyzed for each sample in parallel wells to assess the integrity of the RNA. Primers and probes were obtained from Integrated DNA Technologies as follows: p53for, 5′-GCCAAAGAAGAAACCACTGGATG-3′; p53rev, 5′-TGAGTTCCAAGGCCTCATTCAG-3′; p53probe, 5′-FAM-ATTTCACCCTTCAGATCCGTGGGCGT-TAMRA-3′; p14ARFfor, 5′-TGATGCTACTGAGGAGCCAGC-3′; p14ARFrev, 5′-ACCACCAGCGTGTCCAGGAA-3′; p14ARFprobe, 5′-FAM-ACTCTCACCCGACCCGTGCACGACGCTGC-TAMRA-3′; GAPDHfor, 5′-GAAGGTGAAGGTCGGAGT-3′, GAPDHrev, 5′-GAAGATGGTGATGGGATTTC-3′; and GAPDHprobe, 5′-VIC-CAAGCTTCCCGTTCTCAGCC-TAMRA-3′.

Pulse-chase analysis of p53

Tet-EF cells were plated in 6 cm plates in the presence or absence of doxycycline 3 days prior to analysis. Cells were then preincubated for 1 hr

in methionine/cysteine-free media (with dialyzed FCS) and pulsed with 400 μCi/ml of methionine/cysteine (Tran^{35}S-Label, ICN Biomedicals) for 1 hr. Cells were washed and chased with full media containing 2 mM methionine/2 mM cysteine for the indicated times. Cells were then washed with PBS and lysed in 1 ml RIPA buffer containing protease inhibitors. The entire quantity of lysate was precleared, subjected to immunoprecipitation with anti-p53-conjugated beads (DO-1; Santa Cruz sc-126 AC), and resolved by electrophoresis. Relative p53 levels were determined by phosphor imaging. Relative labeling of the lysates was determined by electrophoresis of 1 μl total lysate (before immunoprecipitation) and phosphor imager analysis. The raw p53 values obtained were corrected for differences in specific labeling between the samples.

Soft agar assays

Cells were seeded at a density of 1×10^5 per 6 cm plate in 0.35% agar in the absence or presence of 2 μg/ml doxycycline, in media containing 20% FCS, Iscove's modification of Eagle's media, penicillin/streptomycin, and glutamine.

Acknowledgments

We thank D. Fisher, S. Armstrong, and H. Widlund for critical reading of the manuscript; members of the Golub lab for useful discussions; C. Ladd, L. Guo, M. Reich, and P. Zhang for assistance with the microarray experiments; H. Widlund for assistance with cell cycle experiments; A. Ferrando for assistance with the real-time quantitative PCR analysis; C.T. Denny for providing the FLAG-epitope-tagged EWS/FLI cDNA and for sharing unpublished data; W. Hahn, R.A. Weinberg, S. Lowe, J.P. Morgenstern, K. Vousden, H. Widlund, and K. Münger for providing cDNAs and vectors; J. Fletcher for EWS-502 cells; and J.-S. Lee and R. Mulligan for 293T cells. We also thank E.S. Lander for scientific insight and for critical resources supported in part by Bristol-Myers Squibb Co. and Affymetrix, Inc. S.L.L. is supported by National Institutes of Health training grant HL07574-20.

Received: February 19, 2002
Revised: April 25, 2002

References

Ambros, I.M., Ambros, P.F., Strehl, S., Kovar, H., Gadner, H., and Salzer-Kuntschik, M. (1991). MIC2 is a specific marker for Ewing's sarcoma and peripheral primitive neuroectodermal tumors. Evidence for a common histogenesis of Ewing's sarcoma and peripheral primitive neuroectodermal tumors from MIC2 expression and specific chromosome aberration. Cancer *67*, 1886–1893.

Arvand, A., Bastians, H., Welford, S.M., Thompson, A.D., Ruderman, J.V., and Denny, C.T. (1998). EWS/FLI1 up regulates mE2-C, a cyclin-selective ubiquitin conjugating enzyme involved in cyclin B destruction. Oncogene *17*, 2039–2045.

Bates, S., Phillips, A.C., Clark, P.A., Stott, F., Peters, G., Ludwig, R.L., and Vousden, K.H. (1998). p14ARF links the tumour suppressors RB and p53. Nature *395*, 124–125.

Damalas, A., Kahan, S., Shtutman, M., Ben-Ze'ev, A., and Oren, M. (2001). Deregulated beta-catenin induces a p53- and ARF-dependent growth arrest and cooperates with Ras in transformation. EMBO J. *20*, 4912–4922.

Dellatre, O., Zucman, J., Plougastel, B., Desmaze, C., Melot, T., Peter, M., Heinrich, K., Houbert, I., de Jong, P., Rouleau, G., et al. (1992). Gene fusion with an *ETS* DNA-binding domain caused by chromosome translocation in human tumours. Nature *359*, 162–165.

Deneen, B., and Denny, C.T. (2001). Loss of p16 pathways stabilizes EWS/FLI1 expression and complements EWS/FLI1 mediated transformation. Oncogene *20*, 6731–6741.

de Stanchina, E., McCurrach, M.E., Zindy, F., Shieh, S., Ferbeyre, G., Samuelson, A.V., Prives, C., Roussel, M.F., Sherr, C.J., and Lowe, S.W. (1998). E1A signaling to p53 involves the p19ARF tumor suppressor. Genes Dev. *12*, 2434–2442.

Fellinger, E.J., Garin-Chesa, P., Triche, T.J., Huvos, A.G., and Rettig, W.J. (1991). Immunohistochemical analysis of Ewing's sarcoma cell surface antigen p30/32MIC2. Am. J. Pathol. *139*, 317–325.

Golub, T.R., Slonim, D.K., Tamayo, P., Huard, C., Gaasenbeek, M., Mesirov, J.P., Coller, H., Loh, M.L., Downing, J.R., Caligiuri, M.A., et al. (1999). Molecular classification of cancer: class discovery and class prediction by gene expression monitoring. Science *286*, 531–537.

Hahn, W.C., Dessain, S.K., Brooks, M.W., King, J.E., Elenbaas, B., Sabatini, D.M., DeCaprio, J.A., and Weinberg, R.A. (2002). Enumeration of the simian virus 40 early region elements necessary for human cell transformation. Mol. Cell. Biol. *22*, 2111–2123.

Haupt, Y., Maya, R., Kazaz, A., and Oren, M. (1997). Mdm2 promotes the rapid degradation of p53. Nature *387*, 296–299.

Khan, J., Wei, J.S., Ringner, M., Saal, L.H., Ladanyi, M., Westermann, F., Berthold, F., Schwab, M., Antonescu, C.R., Peterson, C., and Meltzer, P.S. (2001). Classification and diagnostic prediction of cancers using gene expression profiling and artificial neural networks. Nat. Med. *7*, 673–679.

Kim, J., and Pelletier, J. (1999). Molecular genetics of chromosome translocations involving *EWS* and related family members. Physiol. Genomics *1*, 127–138.

Kovar, H. (1998). Ewing's sarcoma and peripheral primitive neuroectodermal tumors after their genetic union. Curr. Opin. Oncol. *10*, 334–342.

Kovar, H., Auinger, A., Jug, G., Aryee, D., Zoubek, A., Salzer-Kuntschik, M., and Gadner, H. (1993). Narrow spectrum of infrequent p53 mutations and absence of MDM2 amplification in Ewing tumours. Oncogene *8*, 2683–2690.

Kovar, H., Jug, G., Aryee, D., Zoubek, A., Ambros, P., Gruber, B., Windhager, R., and Gadner, H. (1997). Among genes involved in the *RB* dependent cell cycle regulatory cascade, the *p16* tumor suppressor gene is frequently lost in the Ewing family of tumors. Oncogene *15*, 2225–2232.

Kubbutat, M.H., Jones, S.N., and Vousden, K.H. (1997). Regulation of p53 stability by Mdm2. Nature *387*, 299–303.

Ladanyi, M., Lewis, R., Jhanwar, S.C., Gerald, W., Huvos, A.G., and Healey, J.H. (1995). *MDM2* and *CDK4* gene amplification in Ewing's sarcoma. J. Pathol. *175*, 211–217.

Lessnick, S.L., Braun, B.S., Denny, C.T., and May, W.A. (1995). Multiple domains mediate transformation by the Ewing's sarcoma EWS/FLI-1 fusion gene. Oncogene *10*, 423–431.

May, W.A., Gishizky, M.L., Lessnick, S.L., Lunsford, L.B., Lewis, B.C., Delattre, O., Zucman, J., Thomas, G., and Denny, C.T. (1993a). Ewing sarcoma 11;22 translocation produces a chimeric transcription factor that requires the DNA-binding domain encoded by FLI1 for transformation. Proc. Natl. Acad. Sci. USA *90*, 5752–5756.

May, W.A., Lessnick, S.L., Braun, B.S., Klemsz, M., Lewis, B.C., Lunsford, L.B., Hromas, R., and Denny, C.T. (1993b). The Ewing's sarcoma EWS/FLI-1 fusion gene encodes a more potent transcriptional activator and is a more powerful transforming gene than FLI-1. Mol. Cell. Biol. *13*, 7393–7398.

McKeon, C., Thiele, C.J., Ross, R.A., Kwan, M., Triche, T.J., Miser, J.S., and Israel, M.A. (1988). Indistinguishable patterns of protooncogene expression in two distinct but closely related tumors: Ewing's sarcoma and neuroepithelioma. Cancer Res. *48*, 4307–4311.

Morgenstern, J.P., and Land, H. (1990). Advanced mammalian gene transfer: high titre retroviral vectors with multiple drug selection markers and a complementary helper-free packaging cell line. Nucleic Acids Res. *18*, 3587–3596.

Palmero, I., Pantoja, C., and Serrano, M. (1998). p19ARF links the tumour suppressor p53 to Ras. Nature *395*, 125–126.

Patino-Garcia, A., and Sierrasesumaga, L. (1997). Analysis of the p16INK4 and TP53 tumor suppressor genes in bone sarcoma pediatric patients. Cancer Genet. Cytogenet. *98*, 50–55.

Pomerantz, J., Schreiber-Agus, N., Liegeois, N.J., Silverman, A., Alland, L., Chin, L., Potes, J., Chen, K., Orlow, I., Lee, H.W., et al. (1998). The Ink4a tumor suppressor gene product, p19Arf, interacts with MDM2 and neutralizes MDM2's inhibition of p53. Cell *92*, 713–723.

Prendergast, G.C. (1999). Mechanisms of apoptosis by c-Myc. Oncogene *18*, 2967–2987.

Serrano, M., Lin, A.W., McCurrach, M.E., Beach, D., and Lowe, S.W. (1997). Oncogenic *ras* provokes premature cell senescence associated with accumulation of p53 and p16INK4a. Cell *88*, 593–602.

Shaulian, E., Zauberman, A., Ginsberg, D., and Oren, M. (1992). Identification of a minimal transforming domain of p53: negative dominance through abrogation of sequence-specific DNA binding. Mol. Cell. Biol. *12*, 5581–5592.

Sorensen, P.H.B., and Triche, T.J. (1996). Gene fusions encoding chimaeric transcription factors in solid tumors. Semin. Cancer Biol. *7*, 3–14.

Stott, F.J., Bates, S., James, M.C., McConnell, B.B., Starborg, M., Brookes, S., Palmero, I., Ryan, K., Hara, E., Vousden, K.H., and Peters, G. (1998). The alternative product from the human CDKN2A locus, p14(ARF), participates in a regulatory feedback loop with p53 and MDM2. EMBO J. *17*, 5001–5014.

Tamayo, P., Slonim, D., Mesirov, J., Zhu, Q., Kitareewan, S., Dmitrovsky, E., Lander, E.S., and Golub, T.R. (1999). Interpreting patterns of gene expression with self-organizing maps: methods and application to hematopoietic differentiation. Proc. Natl. Acad. Sci. USA *96*, 2907–2912.

Teitell, M.A., Thompson, A.D., Sorensen, P.H., Shimada, H., Triche, T.J., and Denny, C.T. (1999). EWS/ETS fusion genes induce epithelial and neuroectodermal differentiation in NIH 3T3 fibroblasts. Lab. Invest. *79*, 1535–1543.

Vousden, K. (1993). Interactions of human papillomavirus transforming proteins with the products of tumor suppressor genes. FASEB J. *7*, 872–879.

Wei, W., Hemmer, R.M., and Sedivy, J.M. (2001). Role of p14(ARF) in replicative and induced senescence of human fibroblasts. Mol. Cell. Biol. *21*, 6748–6757.

Zhang, Y., Xiong, Y., and Yarbrough, W.G. (1998). ARF promotes MDM2 degradation and stabilizes p53: ARF-INK4a locus deletion impairs both the Rb and p53 tumor suppression pathways. Cell *92*, 725–734.

Zindy, F., Eischen, C.M., Randle, D.H., Kamijo, T., Cleveland, J.L., Sherr, C.J., and Roussel, M.F. (1998). Myc signalling via the ARF tumor suppressor regulates p53-dependent apoptosis and immortalization. Genes Dev. *12*, 2424–2433.